HHS Public Access

Author manuscript

J Vis Lang Comput. Author manuscript; available in PMC 2019 December 11.

Published in final edited form as:

J Vis Lang Comput. 2019 December ; 55: . doi:10.1016/j.cola.2019.100911.

Perceptually guided contrast enhancement based on viewing distance⋆

Liang Zhou[*,a], **Daniel Weiskopf**[b], **Chris R. Johnson**[a]

[a]SCI Institute, University of Utah, United States

[b]Visualization Research Center, University of Stuttgart, Germany

Abstract

We propose an image-space contrast enhancement method for color-encoded visualization. The contrast of an image is enhanced through a perceptually guided approach that interfaces with the user with a single and intuitive parameter of the virtual viewing distance. To this end, we analyze a multiscale contrast model of the input image and test the visibility of bandpass images of all scales at a virtual viewing distance. By adapting weights of bandpass images with a threshold model of spatial vision, this image-based method enhances contrast to compensate for contrast loss caused by viewing the image at a certain distance. Relevant features in the color image can be further emphasized by the user using overcompensation. The weights can be assigned with a simple band-based approach, or with an efficient pixel-based approach that reduces ringing artifacts. The method is efficient and can be integrated into any visualization tool as it is a generic image-based post-processing technique. Using highly diverse datasets, we show the usefulness of perception compensation across a wide range of typical visualizations.

Keywords

Contrast; Visualization; Human visual perception

1. Introduction

A faithful visual representation relies on both appropriate mapping of the data and the visual perception followed [1]. In this paper, we focus on the latter—visual perception in the context of visualizations, and specifically, color encoding of 2D images. In particular, we study the faithfulness of contrast representation impacted by viewing distance. Our new method has the main effect of enhancing contrast depending on virtual viewing distance. This paper is an extended version of our previous method [2] with reuse of materials from

⋆This article was originally submitted to the Journal of Journal of Visual Languages and Computing, however during the process of review the journal underwent a name change and is now titled Journal of Computer Languages.

*Corresponding author. lzhou@sci.utah.edu, liang.zhou@visus.uni-stuttgart.de (L. Zhou).

Supplementary material

Supplementary material associated with this article can be found, in the online version, at doi:10.1016/j.cola.2019.100911.

Declaration of Competing Interest

None.

there. In this work, we extend the method framework with a new per-pixel contrast enhancement method.

Color encoding is one of the main research topics in visualization [3–6]. Here, we refer to color as a combination of achromatic and chromatic information. A large body of research focuses on rules and factors affecting the effectiveness of color coding. The perception of chromatic and achromatic information, together with the effect of spatial frequency and contrast, has been studied [4,5]. However, few papers focus on controllable contrast enhancement methods in the context of visualization—our viewing-distance-based contrast enhancement method is the first one to the best of our knowledge.

Our method is inspired by studies in human visual perception. The basis of our method is a threshold model of spatial vision, i.e., a model that predicts the visibility of an object under different viewing conditions. The computation of contrast and contrast sensitivity functions (CSF) is the core of such a model. It is believed that the human visual system contains visual pathways in a bandpass fashion, and therefore, spatial vision can be appropriately modeled by multiscale models [7–9]. A multiscale contrast model is proposed by Peli [10] to address the contrast representation of a complex image. There, a bandpass image pyramid is built using either cosine-log filters of various scales or multiscale Gaussian filters. We adopt this contrast representation [10] and choose to use the cosine-log pyramid as it provides more accurate spatial frequencies.

CSFs have been measured in physiological and psychophysical experiments [7,11–13]. These measurements are successfully matched by computational models of CSFs. In particular, Daly [14] proposes a computational model for multiscale CSFs to predict visible differences between two images. This comprehensive model considers variables affecting the contrast sensitivity, including the illumination level, image size, stimuli orientation, and viewing distance. Our contrast enhancement method combines the multiscale contrast model [10] with the computational CSF [14]. A virtual viewing distance is used as the single parameter to enhance contrast so that all bandpass images become visible.

Two weight assignment approaches are supported in our method: a band-based method that adjusts weights for bandpass images globally; and a pixel-based method that allows for setting weights for individual pixels of bandpass images.

Mullen [13] studies visual sensitivity for sinusoidal grating patterns for monochromatic luminance gratings and isoluminant chromatic gratings. The CSFs from experiments show that better visual sensitivity is achieved for chromatic channels for low spatial frequency stimuli, whereas the luminance channel provides better sensitivity for stimuli with higher spatial frequency. Therefore, we keep the chromatic channels for low spatial frequencies and use the viewing distance-adjusted achromatic image to provide more insights into higher spatial frequencies. An example of an MRI brain dataset is shown as the original (Fig. 1(a)), enhanced by our band-based method (Fig. 1(b)), and enhanced by our pixel-based method (Fig. 1(c)). The enhanced results show details inside the brain tissues that look washed away in the original visualization.

The contribution of our work is an efficient image-based technique that improves contrast using a single parameter of virtual viewing distance. The method is inspired by the perception literature, and it goes beyond just compensation for contrast loss caused by viewing distance but allows for flexible overcompensation to emphasize relevant features in the image.

One benefit of our approach is its generality: our method can be used for a wide range of visualization examples, ranging from volume visualization with transfer functions all the way to 2D geographic information visualization, as demonstrated in our examples. Another advantage is the simplicity of the image-based post-processing that does not interfere with previous steps in the visualization pipeline and can be combined with any visualization system. Through our efficient computational model, the image enhancement works in interactive settings. Our method comes with easy and intuitive controllability with the virtual viewing distance as the only parameter.

2. Related work

Utilizing color in computer-based visualization is an important research topic [6]. Luminance and spatial frequency aspects in visualizations with color mapping are in particular related to our work. Specifically, luminance is more effective for revealing high-spatial-frequency structures than chromatic channels [4,15]. The spatial frequency of the data is considered an important factor in color map design [5]. Color maps and high-frequency sinusoid gratings are combined to design better perceptually uniform color maps that have good luminance contrast across the whole range [16].

Luminance also plays an important role in improving details in natural image processing. Tone mapping operators [17–19] are concerned with the compression of the luminance range while preserving perceived contrast. Unlike our proposed method, these are image-processing methods that target to reproduce the perceived image of high dynamic range input on low dynamic range devices, and cannot be tuned with a viewing distance.

Computational perception models exist, albeit outside of the field of visualization. Daly [14] predicts the visible differences between two images by devising a computational visual perception model. We make use of the CSF of [14] for threshold contrast computation in our method. The high dynamic range (HDR) visible difference predictor (HDR VDP) [20] is a perceptual model that compares a test high dynamic range image against a reference high dynamic range image and predicts the visibility, i.e., the visible differences between these images, and quality—the quality degradation with respect to the reference image. However, these models focus on generating image metric for natural-scened photos or synthesized images, whereas our method perceptually enhances potentially abstract visualizations.

In the context of visualization, perceptual aspects have been studied. The spectral visualization sharpening [21] method is closely related to this work. That method [21] also enhances the contrast of visualization images with a viewing distance parameter but is based on a spectral model of vision. This spectral model could simulate perceptual effects due to the change of viewing distance and contrast enhancement is achieved by inverting weights in

this model. Our paper is concerned with color perception in the context of its spatial embedding, and the paper by Isenberg et al. [22] is relevant to our work but with a different goal in mind. Isenberg et al. study the visibility of features of different spatial frequencies at different viewing distances of a display wall. They propose a hybrid-image method that combines a near image containing high-frequency information with a far image that has low-frequency information to allow the user to perceive coarse features well at distance and acquire fine details when close to the display. We also analyze multiscale band-limited images, however, we utilize them to compensate for perception distortions and design perceptually oriented color transformation. Moreover, rather than a display-wall setting where the user moves back and forth [22], we focus on a typical working space setting where the user sits in front of a regular monitor at more or less a fixed distance.

In regard to compensation for perception effects, there are methods [23,24] that compensate for the simultaneous contrast effect, which makes regions of the same color look different. The compensation is realized by rendering these regions with different colors based on a customized color appearance model. Unlike their work, our method does not focus on the isolated simultaneous contrast effect but how viewing distance affects the contrast on different spatial scales. Furthermore, our method goes beyond compensation but also supports overcompensation, which is important for visualization.

Contrast enhancement or image sharpening is well studied in image processing [25]. An efficient and accurate image sharpener is critical for high-quality image super resolution technique [26] that generates high-resolution output from a single low-resolution input image. However, these techniques are not perceptually-driven and cannot be controlled by the user.

Sufficient contrast is vital for gaining insights into the underlying data in a visualization. In fact, user studies [27] have shown that sharp boundaries created by binning continuous encodings help with the understanding of the data: participants with binned encoding outperform those with continuous encoding in terms of both the completion time and accuracy. Therefore, it is natural to enhance contrast for visualization images. Our method supports flexible interactive overcompensation through a slider, allowing for highlighting features of interest in visualization. It is important to note that such overcompensation is not arbitrary but perceptually-based in our method.

3. Contrast enhancement framework

The input of our method is a color image $f(x, y)$. An image pyramid containing band-limited images $a_i(x, y)$ is extracted using cosine-log filters from the luminance image $f_Y(x, y)$ of $f(x, y)$. Then, contrast images c_i of these band-limited images are calculated, and band weights $\bar{c}_i$ —the averaged values of c_i—are also computed. Next, the core step—viewing-distance-based band weight assignment, which is elaborated in Section 4—is achieved by testing the contrast, i.e., $\bar{c}_i$ for the band-based method and c_i for the pixel-based method, against a CSF S, which is computed separately and independent of the dataset, for a given virtual viewing distance set by the user. The luminance difference image $f_L(x, y)$ is then created by modulating the band weights with $a_i(x, y)$. The final visualization $f_Y(x, y)$ is created by

combining the luminance difference image $f_L(x, y)$ and the chromatic part $f_C(x, y)$ of $f(x, y)$. The workflow of our method is illustrated in Fig. 2. The remainder of this section explains each module in our pipeline, and the two virtual viewing-distance-based weight assignment methods will be detailed in Section 4.

3.1. Image pyramid generation

A multiscale model of spatial vision uses an image pyramid generated from the input image. An image $f(x, y)$ can be described in the frequency domain with polar coordinates representation:

$$\begin{aligned} F(u,v) = F(r,\theta) &= L_0(r,\theta) + \sum_{i=1}^{l-1} A_i(r,\theta) + H_l(r,\theta), \\ &\approx L_0(r,\theta) + \sum_{i=1}^{l-1} A_i(r,\theta), \\ r = \sqrt{u^2+v^2}, &\theta = \arctan\left(\frac{v}{u}\right), \end{aligned} \tag{1}$$

where u and v are the horizontal and vertical spatial frequency co-ordinates in cycles/image [10] (the image is always zero-padded to be squared with the side of power of 2), r and θ are the polar spatial frequency coordinates, L_0 and H_l are low and highpass residuals respectively, l is the level of the pyramid, and A_i are band-limited images in the frequency domain. An image can be approximated without the high-frequency residual [10]; we, therefore, discard the high-frequency image. The band-limited images are created by filtering $F(r, \theta)$ by multiplying a bandpass filter $G_i(r)$:

$$A_i(r,\theta) = F(r,\theta)G_i(r)\,. \tag{2}$$

A popular choice of G_i is Gaussian filters with various standard deviations. Gaussian filters are closely related to scale space [28] and are widely used in imaging and computer vision. The advantage is that they can be conveniently transformed between the spatial domain and frequency domain. However, the Gaussian filters are asymmetrical in the logarithmic frequency domain, and reconstruction of the input image is nontrivial as filters do not sum to one [10].

Instead, we adopt the cosine-log filter bank [10] for image pyramid generation. We use a cosine-log filter of 1-octave width, i.e., the central spatial frequency is twice the frequency of the lower cutoff frequency and half of the higher cutoff frequency, centered at frequency 2^i cycles/image:

$$G_i(r) = 0.5[1 + \cos(\pi \log_2 r - \pi i)\ ]. \tag{3}$$

Fig. 3 shows a 1D example of a cosine-log filter bank comprised of 1-octave-wide cosine-log filters. The shapes are symmetrical in the log spatial frequency axis and the summation of filter responses equals to 1 as shown by the red dash curve. In practice, these filters are defined in the discrete frequency domain and the first few levels occupy only a few pixels.

The cosine functions are not accurately represented there. As a result, we slightly change the filter weights at these pixels to make sure that the summation of all filters equals to one, as can be seen in Fig. 3.

Bandpass images in the spatial domain $a_i(x, y)$ are obtained by applying the inverse Fourier transform to $A_i(u, v)$. Fig. 4 shows an image pyramid of 8 levels of the Hurricane Isabel data [29]. It can be seen that the cosine-log filters capture features of different spatial frequencies in the image.

3.2. Contrast computation

The average contrast of each bandpass image $a_i(x, y)$ is calculated and later tested against the threshold contrast given by the CSF, which is discussed in the next section. We follow the approach of Peli [10] obtain contrast images $c_i(x, y)$ of each pyramid level:

$$c_i(x,y) = \frac{a_i(x,y)}{l_i(x,y)}, \qquad l_i(x,y) = l_0(x,y) + \sum_{j=1}^{i-1} a_j(x,y), \tag{4}$$

where $l_0(x, y)$ is the lowpass residual image in the spatial domain ($L_0(r, \theta)$ in the polar coordinates frequency domain), and $l_i(x, y)$ is the low-pass image before the ith level.

The per-pixel representation $c_i(x, y)$ is used as contrast for our pixel-based method (Section 4.2) as in Peli's approach [10], we further compute an average contrast $\bar{c}_i$ for level i for the band-based method (Section 4.1). Therefore, we calculate the average band contrast $\bar{c}_i$ for band i:

$$\overline{c_i} = \frac{\sum_{c_i(x,y) \neq 0} |c_i(x,y)|}{\sum_{c_i(x,y) \neq 0} 1}. \tag{5}$$

Note that other contrast definitions can also be used in our framework.

3.3. CSF and threshold contrast

The Daly CSF [14] is a comprehensive computational CSF model including many parameters: $S(r, \theta, L, i^2, d, e)$, where r is the radial spatial frequency in cycles/degree (cpd), θ is the orientation, L is the illumination level, i^2 is the image size in degrees, d is the distance for lens accommodation, and e is eccentricity. Fig. 5 shows Daly CSFs with various illumination levels L; there, the shape of CSFs varies significantly for different L: higher illumination levels offer better contrast sensitivity; CSF changes from lowpass to bandpass with increasing illumination level. We choose $L = 100$ cd m^{-2}, which is a typical light condition in an office setting, which is our target environment; $d = 0.7$ m is chosen as it is a typical viewing distance in the office setting; e is set to 0 as we assume no eccentricity. Parameters L and i^2 are fixed for a given input image.

Given the CSF, the threshold contrast $c_t(r)$ is simply the inverse of sensitivity S:

$$c_t(r) = \frac{1}{S(r, \theta, 100, i^2, 0.7, 0)}. \quad (6)$$

Note that the orientation θ plays a secondary role for band-based weight assignment (Section 4.1), and, therefore, is set to a constant (0); however, θ is important in pixel-based weight assignment (Section 4.2)—it has to be set based on the image gradient.

3.4. Virtual viewing distance-based weight assignment

The perceptual spatial frequency $r_p(i)$ in cycles/degree of bands are changed in our method through a virtual viewing distance parameter d_v. The cosine-log filter bank gives spatial frequency $r_c(i)$ of each band in cycles/image, and can be converted into the perceptual spatial frequency using:

$$\begin{aligned} r_p(i) &= r_c(i) \cdot s_{deg}(I), i = 0, 1, \ldots, l-1, \\ s_{deg}(I) &= 2 \cdot \frac{180}{\pi} \arctan\left(0.5 \frac{s_{cm}(I)}{d_v}\right), \end{aligned} \quad (7)$$

where l is the number of layers of the image pyramid, $s_{deg}(I)$ and $s_{cm}(I)$ are angle size in degree and physical size in cm of the image I respectively. The physical size $s_{cm}(I)$ can be calculated given the pixel resolution of the imageas well as the pixel resolution and physical size of the monitor.

Fig. 6 shows the average band contrast curves of an image with different viewing distances (dashed curves) together with a threshold contrast curve generated by the Daly CSF (the blue curve). It can be seen that with increasing virtual viewing distance, the spatial frequency of bands is increased. Our method allows for convenient spatial frequency modification of band-limited images with a single virtual viewing distance parameter. Based on this observation, we propose two approaches for weight assignment and explain them in detail in Section 4.

3.5. Combining image channels

The luminance difference image $f_L(x, y)$ is generated as the weighted sum of band-limited images:

$$f_L(x, y) = \sum_{i=1}^{l-1} w_i \cdot a_i(x, y). \quad (8)$$

The final visualization $f_V(x, y)$ is created by combining $f_L(x, y)$ with the color image $f_C(x, y)$. We replace the achromatic channel $L(f_C(x, y))$ of $f_C(x, y)$ by $L(f_C(x, y)) + f_L(x, y)$, and keep the chromatic channels of $f_C(x, y)$ intact.

Care must be taken when band weights are high as the modified achromatic image become saturated, i.e., fully white or black. Since we would like to preserve the appearance of $f_C(x,$

y) as much as possible, we clamp the achromatic channel $L(f_V(x, y))$ empirically by ± 20% of the luminance of $f_C(x, y)$ to give an appropriate look of the visualization:

$$L(f_V(x,y)): = \min(\max(L(f_V(x,y)), 0.8L(f_C(x,y))), 1.2L(f_C(x,y))) \ .$$

In our current implementation, the combination operation happens in the HSL color space, and the combined color is transformed to the sRGB color space for display.

4. Weight assignment methods

Based on the threshold model of spatial vision, a threshold contrast curve predicts the visibility of features of specific spatial frequency: a feature is not visible if its contrast is below the curve, and it is visible if its contrast sits on or above the curve. The goal of our virtual viewing-distance-based weight assignment is to amplify features so that they become visible given their spatial frequencies set using the virtual viewing distance.

4.1. Band-based weight assignment

Band weight assignment is realized by comparing the average band contrast at virtual perceptual spatial frequencies against the threshold contrast curve. The weight of a band is set to 0, if the band contrast is above the curve; otherwise, the weight is set to be the multiplier that "lifts" the band contrast up to the threshold contrast:

$$w_i = \begin{cases} c_t(r_p(i))/\overline{c_i} - 1, & c_t(r_p(i)) > \overline{c_i} \\ 0 \qquad\qquad\quad , & c_t(r_p(i)) \le \overline{c_i} \end{cases}. \tag{9}$$

It can be seen in Fig. 6 that with a short viewing distance, more bands of low spatial frequencies need to be compensated and higher weights are required for shorter viewing distance, e.g., d_v = 0.2 m; with a long viewing distance, more bands of high spatial frequencies need to be compensated and higher weights are necessary for longer viewing distance (d_v = 2.2 m); bands with medium spatial frequency typically do not require compensation as threshold contrast is very low for these frequencies, i.e., the contrast sensitivity is very high. These findings successfully match our own experiences in daily life.

4.2. Pixel-based weight assignment

The aforementioned band-based method uniformly amplifies whole bandpass images without the consideration of contrast differences within each band. A shortcoming of this global approach is that some features that are clearly visible become over-exaggerated, whereas some other features do not have enough weights to be seen clearly. Therefore, we propose a pixel-based contrast enhancement extension to address this issue. The pixel-based contrast enhancement pipeline remains largely the same as the band-based method except that the pixel-based method uses contrast images rather than averaged band contrast, and weights are set on a per-pixel basis as shown in Fig. 2. The workflow of the weight assignment of the pixel-based contrast enhancement is illustrated in Fig. 7. In the remainder of this section, we explain each step in Fig. 7 in detail.

The effect of orientation (θ) cannot be ignored when testing fine-grain stimuli, e.g., pixel-sized, with the Daly CSF [14], and therefore, it is computationally expensive as the CSF has to be computed for each pixel of each band. In the perception simulation method [9], the contrast transducer functions are modeled to resemble CSF-like behaviors and are used as a unified approximation to threshold spatial vision and suprathreshold vision. Therefore, we adopt the contrast transducer functions for the achromatic channel from Pattanaik et al. [9] as we use the luminance channel for contrast enhancement and compute Eq. (7) only when necessary. The contrast transducer functions read:

$$T(c) = \begin{cases} 22.4(c/0.536)^{0.5}, & c \geq 0.536\,, \\ 22.4(c/0.536)^{p}\,, & \text{otherwise}, \end{cases} \tag{10}$$

where c is the contrast, and the value of p depending on the spatial frequency is summarized in Table 1.

The values of p for peak frequency of 0.5 through 16.0 cpd in Table 1 are adapted from Pattanaik et al. [9], while for 32 cpd, the value of p is calculated by finding the threshold contrast $c_t(r)$ for $r = 32$ with the Daly CSF and then letting $T(c_t(r)) = 1$, i.e., $p = \frac{\log(1/22.4)}{\log(c_t(32)/0.536)}$. Linear interpolation is used to calculate p if the peak frequency of the band is between the values listed in Table 1.

Eq. (10) provides a light-weight alternative to the threshold contrast test—if $T(c) < 1$, the contrast of the pixel is below the threshold and needs to be compensated; otherwise, the contrast is above threshold and the pixel could be seen, and we set the weight of the pixel to 0. Then, the CSF is only computed in cases that a pixel needs to be compensated, and the orientation of the feature can be calculated using the gradient of the contrast image:

$$\theta = \arctan\left(\frac{dc_i(x,y)}{dy}, \frac{dc_i(x,y)}{dx}\right).$$

We use the contrast transducer functions for spatial frequencies up to 32 cpd as there is evidence that the maximum spatial frequency of a perceivable achromatic stimuli is around 30 cpd due to limits of human visual acuity [9], and in our case, we set the cutoff to 32 cpd to correspond with the cosine-log filters. Note that the spatial frequency can go beyond 32 cpd with our method as a long virtual viewing distance can be set for overcompensation, and in that case, the CSF has to be computed for each pixel of bands that have spatial frequencies greater than 32 cpd.

The contrast of pixels of a band may vary significantly and result in contrast-enhanced images with unnatural look—some pixels may become too dark or bright. To avoid such problems, we empirically clamp the weight of a pixel by the smaller value of $c_t(r_p(i), \theta)/c_t(x, y) - 1$—the multiplier that "lifts" the contrast of the pixel to the threshold contrast, and $c_t(r_p(i))/\bar{c}_i - 1$—the average amplitude of the whole band. Therefore, the per-pixel weight assignment mechanism can be described by:

$$w_i(x,y) = \begin{cases} 0\,, & \text{if } T(c_i(x,y)) \geq 1\,, \\ \min\left(\dfrac{c_t(r_p(i),\theta)}{c_i(x,y)}\,, \dfrac{c_t(r_p(i))}{\overline{c_i}}\right) - 1\,, & \text{if } T(c_i(x,y)) < 1. \end{cases} \tag{11}$$

The per-pixel compensated results can be found in Figs. 1, 8, 9, and 10. In general, compared to the band-based method, pixel-based contrast-enhanced images better preserve features in the original images while generating less ringing artifacts.

5. User interaction and implementation

The virtual viewing distance visualization method has only one parameter—the virtual viewing distance d_v. Therefore, user interaction is simple and intuitive with our method as d_v can be easily controlled by a single slider.

The method is implemented in our visualization tool written in C + + using Qt and OpenGL. Our tool supports both 2D images and 3D volume datasets. The cosine-log filter bank is computed only once for an image or a slice of a volume dataset when its size was changed. The image pyramid is computed by Fourier transform using an efficient fast Fourier transform implementation in OpenCV. Contrast image generation is also aided by OpenCV. The computation of these steps takes up to a few seconds depending on the size of the image.

Interactivity is achieved with our implementation with the help of GPU acceleration. For the band-based method, the CSF is computed once and stored in a lookup table, and weight assignment involves only a few lookups and divisions. The resulting band weights are passed to the GPU, and the luminance image was combined with the color image in an OpenGL Shading Language (GLSL) shader to give the final visualization. Whereas for the pixel-based method, another GLSL shader calculates the contrast transducer function for each pixel and combines the per-pixel weighted luminance image with the color image; this shader also computes the orientation of the stimuli, and the CSF when the pixel's contrast is considered below-threshold after the contrast transducer function test. Note that in the pixel-based mode, we use only the top 5 high-frequency bandpass images to avoid artifacts caused by features of much lower frequencies that pass the contrast transducer function test. A code snippet of the GLSL shader is provided in the supplemental material for reproducibility.

6. Examples

The usefulness of our perceptual enhancement is demonstrated through various datasets of different types in this section. Examples range from color mapping on 2D images (slices) to show scalar fields of atmosphere simulation, brain MRI imaging, 3D volume rendered image, all the way to 2D geographic information visualization on maps. Insets of zoom-ins are provided in all example figures for a clearer comparison between the original, band-based contrast-enhanced, and pixel-based contrast-enhanced images.

6.1. Hurricane Isabel

The Hurricane Isabel simulation data is shown in Fig. 8. Here, we see the pressure attribute of time step 29, which well demonstrates the nature of atmosphere simulations that have large-scale smooth, homogeneous structures with subtle yet important vortex details. With a spectrum color map from ColorBrewer[1], we are able to roughly see the hurricane eye, the spiral arms, and the shore area in the original color-mapped visualization. Details of both the hurricane eye and spiral arm structures can be better seen with a viewing distance of 200 cm with the band-based method (Fig. 8(b)). However, the band-based contrast-enhanced image reduces the resolution of fine features in the data and gives a slightly blurry look due to the ringing artifact. With our pixel-based method (Fig. 8(c)), the contrast of fine details throughout the image is enhanced, yet the resolution of these features are better preserved compared to the band-based method in Fig. 8(b).

6.2. MRI Brain

Results of an MRI brain scan are shown in Fig. 1. The dataset is visualized with a slightly modified isoluminant color map [32]. Without enhancement, the image gives a washed away impression that the brain cannot be easily separated from the surrounding tissues (cyan), and the delicate folded details are not recognizable without difficulty. With a virtual viewing distance of 100 cm, the brain structure with fine details become clearly noticeable with the band-based weight assignment method, especially for the cerebellum (Fig. 1(b)). Applying the pixel-based method to the data (Fig. 1 (c)), structure boundaries are enhanced with finer curves, and the result looks more natural than the image enhanced with the band-based method (Fig. 1(b)).

6.3. Volume rendered images

Fig. 9 (row 1) shows volume renderings of a supernova simulation using an ambient scattering model [30]. The perceptually enhanced result using the band-based method (Fig. 9(b)) provides a less blurry visualization compared to the original rendering (Fig. 9(a)). Specifically, boundaries of complex vortex structures become more prominent with the enhanced contrast, making it easier to gain insights into these structures. The pixel-based method (Fig. 9(c)) gives a result where high-frequency features are more subtly enhanced compared to Fig. 9(b).

Fig. 9 (row 2) shows volume renderings with Phong shading of a simulation of a heptane pool fire. With our band-based method (Fig. 9(e)), the contrast of boundaries of layers of the fire is enhanced providing better depth cues than the original (Fig. 9(d)). In comparison, the pixel-based method generates a more subtly enhanced image with less ringing artifacts (Fig. 9(f)) than the band-based method.

6.4. GIS data

Fig. 10 shows a visualization of movement behavior [31] on a GIS city dataset. The visualization is designed to achieve a focus-and-context effect: the focus is on dark red road

[1] http://colorbrewer2.org.

networks and the region inside the circle area, other regions are given reduced contrast. The perceptually enhanced result (Fig. 10(b)) improves the overall contrast of the visualization while preserving the focus-and-context feeling. Icons and structures inside the circle of focus become more prominent. Details outside the focus are enhanced so that more insights can be gained easily; nevertheless, the enhancement is not too strong to distract users from the focus region. However, ringing artifacts can be seen in Fig. 10(b), especially around the circle of focus, and inside the icons. Fig. 10(c) shows the result using the pixel-based method—the ringing artifacts are reduced compared to Fig. 10(b), while the contrast of the whole image is enhanced compared to the original (Fig. 10(a)).

7. Quantitative evaluation

Our method is evaluated quantitatively using the Blind/Referenceless Image Spatial Quality Evaluator (BRISQUE) [33], where a lower score indicates better perceived quality. The scores for the original image s_0, band-enhanced image s_{be}, and per-pixel-enhanced image s_{pe}, respectively, are summarized in Table 2. Furthermore, we calculate the structural similarity index [34] comparing the original image against the band-enhanced result i_{be} and the per-pixel-enhanced result i_{pe}. As shown in Table 2, in general, the perceived quality of images is improved using our contrast enhancement method except for the GIS dataset. The GIS dataset is very different from other examples in nature and contains mostly high-frequency features—it shows the limits of our method, which is best used for color-mapped scientific visualizations; however, the numbers are still comparable here. Higher values are shown for i_{pe} than i_{be}, indicating that the pixel-based method yields images that look more similar to the original than the band-based method—this is in line with our observation that the enhancements with the former are more subtle than the latter.

Overall, the quantitative metrics is another indicator showing the effectiveness of our method.

8. Conclusions and future work

In this paper, we have introduced a contrast enhancement method based on virtual viewing distance for data visualization with color images. The perceptually based enhancement is achieved by adjusting bands that are extracted from the luminance channel of the input image to become visible at a virtual viewing distance. Specifically, the method is built on a multiscale image pyramid created with cosine-log filters; weights of band-limited images are assigned by testing average band contrast against a threshold contrast curve derived from a CSF. To reduce the potential ringing artifacts, we have further extended our method with an efficient pixel-based contrast enhancement approach—there, the weight of each pixel in each band-limited image is set using a hybrid method that combines the CSF and contrast transducer functions. The pixel-based method is recommended for high-quality renderings with subtle enhancements, whereas the band-based method is recommended for more controllability and drastic effects. Our technique has only a single parameter—virtual viewing distance that can be tuned easily by a slider. Interactivity is achieved with our implementation. The proposed method can be integrated into any visualization pipeline as image post-processing. A wide range of datasets that have representative image features is

shown as examples to demonstrate the usefulness of our method. Our viewing distance visualization method is a potential technique that benefits any visualization with effective perceptual enhancement.

In the future, we would like to conduct quantitative user studies to understand the optimal setting of virtual viewing distance for different datasets. Furthermore, the method could be extended to a VR/AR environment, where the virtual viewing distance can be set using sensors to achieve a more natural way of user interaction.

Acknowledgement

This work is funded by the Deutsche Forschungsgemeinschaft (DFG, German Research Foundation) within SFB 716 D.5 and Project-ID 251654672 – TRR 161, by National Institute of General Medical Sciences of the National Institutes of Health under grant number P41 GM103545-18, and by the Intel Graphics and Visualization Institutes. The GPU used for this research was donated by the Nvidia Corporation. This work reuses materials from the ACM VINCI paper [2] with permission, © ACM.

References

[1]. Nguyen Q, Eades P, Hong SH, On the faithfulness of graph visualizations, Proceedings of the 2013 IEEE Pacific Visualization Symposium, PacificVis'13, (2013), pp. 209–216, 10.1109/PacificVis.2013.6596147.

[2]. Zhou L, Weiskopf D, Contrast enhancement based on viewing distance, Proceedings of the Eleventh International Symposium on Visual Information Communication and Interaction, VINCI' 18, (2018), pp. 25–32, 10.1145/3231622.3231628.

[3]. Trumbo BE, A theory for coloring bivariate statistical maps, Am. Stat. 35 (4) (1981) 220–226, 10.1080/00031305.1981.10479360.

[4]. Ware C, Color sequences for univariate maps: theory, experiments and principles, IEEE Comput. Graph. Appl. 8 (5) (1988) 41–49, 10.1109/38.7760.

[5]. Bergman L, Rogowitz B, Treinish L, A rule-based tool for assisting colormap selection, Proceedings of IEEE Conference on Visualization '95, (1995), pp. 118–125, 10.1109/VISUAL.1995.480803.

[6]. Zhou L, Hansen CD, A survey of colormaps in visualization, IEEE Trans. Vis. Comput. Graph. 22 (8) (2016) 2051–2069, 10.1109/TVCG.2015.2489649. [PubMed: 26513793]

[7]. Wilson HR, Psychophysical models of spatial vision and hyperacuity, Spat. Vis. 10 (1991) 64–81.

[8]. Watson AB, Solomon JA, Model of visual contrast gain control and pattern masking, J. Opt. Soc. Am. A 14 (9) (1997) 2379–2391, 10.1364/JOSAA.14.002379.

[9]. Pattanaik SN, Ferwerda JA, Fairchild MD, Greenberg DP, A multiscale model of adaptation and spatial vision for realistic image display, Proceedings of the Twenty-fifth Annual Conference on Computer Graphics and Interactive Techniques, SIGGRAPH '98, (1998), pp. 287–298, 10.1145/280814.280922.

[10]. Peli E, Contrast in complex images, J. Opt. Soc. Am. A 7 (10) (1990) 2032–2040, 10.1364/JOSAA.7-002032. [PubMed: 2231113]

[11]. Nes FLV, Bouman MA, Spatial modulation transfer in the human eye, J. Opt. Soc. Am. 57 (3) (1967) 401–406, 10.1364/JOSA.57.000401.

[12]. Campbell FW, Robson JG, Application of fourier analysis to the visibility of gratings, J. Physiol. (Lond.) 197(3) 551–566. doi:10.1113/jphysiol.1968.sp008574.

[13]. Mullen KT, The contrast sensitivity of human colour vision to red-green and blue-yellow chromatic gratings, J. Physiol. (Lond.) 359(1) 381–400. doi:10.1113/jphysiol.1985.sp015591.

[14]. Daly SJ, Visible differences predictor: an algorithm for the assessment of image fidelity, 1992, doi:10.1117/12.135952.

[15]. Rogowitz BE, Treinish LA, Bryson S, How not to lie with visualization, Comput. Phys. 10 (3) (1996) 268–273, https://doi.Org/10.1063/1.4822401.

[16]. Kovesi P, Good colour maps: how to design them, CoRR abs/1509.03700 (2015).

[17]. Reinhard E, Stark M, Shirley P, Ferwerda J, Photographic tone reproduction for digital images, ACM Trans. Graph. 21 (3) (2002) 267–276, 10.1145/566654.566575.

[18]. Fattal R, Lischinski D, Werman M, Gradient domain high dynamic range compression, ACM Trans. Graph. 21 (3) (2002) 249–256, 10.1145/566654.566573.

[19]. Mai Z, Mansour H, Mantiuk R, Nasiopoulos P, Ward R, Heidrich W, Optimizing a tone curve for backward-compatible high dynamic range image and video compression, IEEE Trans. Image Process. 20 (6) (2011) 1558–1571, 10.1109/TIP.2010.2095866. [PubMed: 21134816]

[20]. Mantiuk R, Kim KJ, Rempel AG, Heidrich W, HDR-VDP-2: A calibrated visual metric for visibility and quality predictions in all luminance conditions, ACM Trans. Graph. 30 (4) (2011) 40:1–40:14, 10.1145/2010324.1964935.

[21]. Zhou L, Netzel R, Weiskopf D, Johnson CR, Spectral visualization sharpening, ACM Symposium on Applied Perception 2019 (SAP '9), ACM, New York, NY, USA, 2011, pp. 18:1–18:9, 10.1145/3343036.3343133.

[22]. Isenberg P, Dragicevic P, Willett W, Bezerianos A, Fekete J-D, Hybrid-image visualization for large viewing environments, IEEE Trans. Vis. Comput. Graph. 19 (12) (2013) 2346–2355, 10.1109/TVCG.2013.163. [PubMed: 24051801]

[23]. Mittelstädt S Stoffel A Keim DA, Methods for compensating contrast effects in information visualization, Comput. Graph. Forum 33 (3) (2014) 231–240, 10.1111/cgf.12379.

[24]. Mittelstädt S, Keim DA, Efficient contrast effect compensation with personalized perception models, Comput. Graph. Forum 34 (3) (2015) 211–220, 10.1111/cgf.12633.

[25]. Gonzalez RC, Woods RE, Digital Image Processing, (3rd ed.), Prentice-Hall, Inc, Upper Saddle River, NJ, USA 2006.

[26]. Romano Y, Isidoro J, Milanfar P, RAISR: Rapid and accurate image super resolution, IEEE Trans. Comput. Imaging 3 (1) (2017) 110–125, 10.1109/TCI.2016.2629284.

[27]. Padilla L, Quinan PS, Meyer M, Creem-Regehr SH, Evaluating the impact of binning 2D scalar fields, IEEE Trans. Vis. Comput. Graph. 23 (1) (2017) 431–440, 10.1109/TVCG.2016.2599106. [PubMed: 27875159]

[28]. Lindeberg T, Feature detection with automatic scale selection, Int. J. Comput. Vis. 30 (2) (1998) 79–116, https://doi.Org/10.1023/A:1008045108935.

[29]. IEEE, IEEE Visualization 2004 Contest data set, 2004, http://vis.computer.org/vis2004contest/data.html.

[30]. Ament M, Sadlo F, Weiskopf D, Ambient volume scattering, IEEE Trans. Vis. Comput. Graph. 19 (12) (2013) 2936–2945, 10.1109/TVCG.2013.129. [PubMed: 24051861]

[31]. Krueger R, Thom D, Ertl T, Visual analysis of movement behavior using web data for context enrichment, Proceedings of the 2014 IEEE Pacific Visualization Symposium, PacificVis'14, (2014), pp. 193–200, 10.1109/PacificVis.2014.57.

[32]. Kindlmann G, Reinhard E, Creem S, Face-based luminance matching for perceptual colormap generation, Proceedings of IEEE Conference on Visualization'O2, (2002), pp. 299–306, 10.1109/VISUAL.2002.1183788.

[33]. Mittal A, Moorthy AK, Bovik AC, No-reference image quality assessment in the spatial domain, IEEE Trans. Image Process. 21 (12) (2012) 4695–4708, 10.1109/TIP.2012.2214050. [PubMed: 22910118]

[34]. Wang Z, Bovik AC, Sheikh HR, Simoncelli EP, Image quality assessment: from error visibility to structural similarity, IEEE Trans. Image Process. 13 (4) (2004) 600–612, 10.1109/TIP.2003.819861. [PubMed: 15376593]

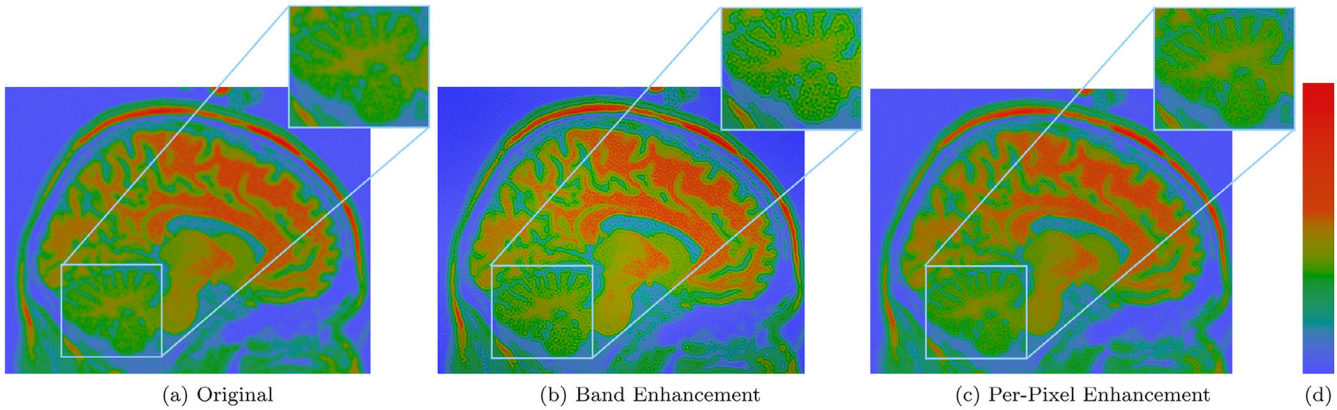

Fig. 1.

Visualizations of the MRI brain dataset with an isoluminant color map (d): (a) original, (b) contrast-enhanced by our band-based method, and (c) contrast-enhanced by the pixel-based method. Zoomed-in details can be seen in insets. Note that all figures in the paper are supposed to be shown on the screen with the longer side of around 30 cm and viewed at around 80 cm away.

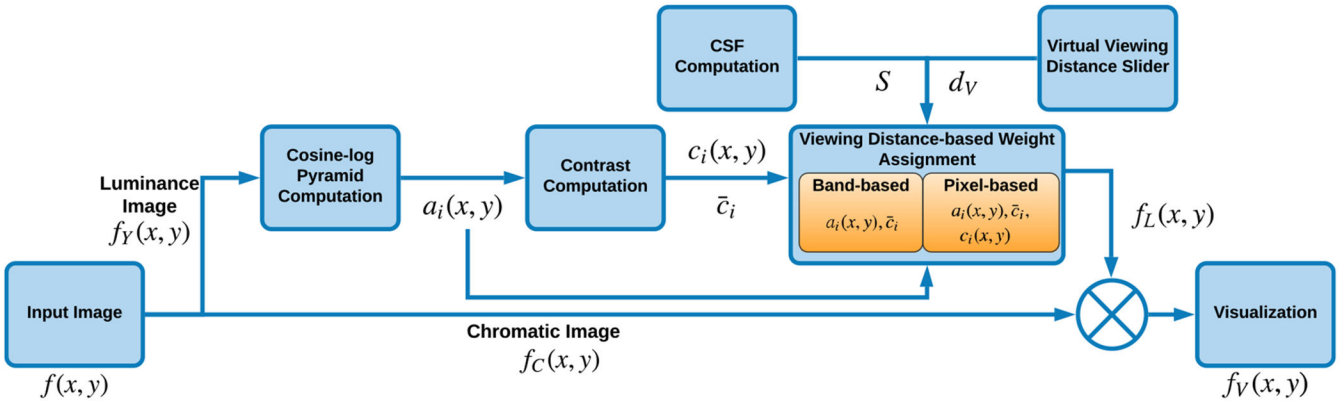

Fig. 2.

The workflow of our contrast enhancement method based on virtual viewing distance.

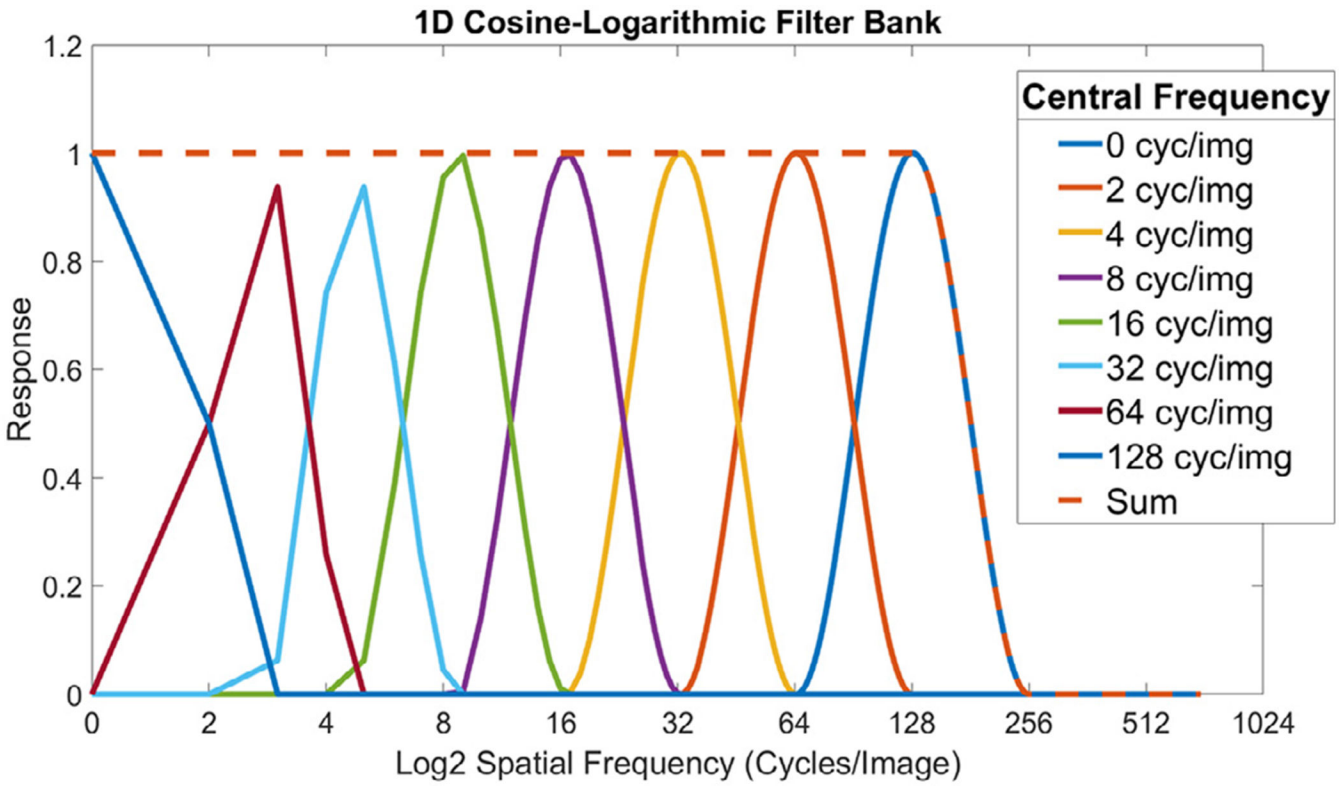

Fig. 3.

Filter bank of 1-octave-wide cosine-log 1D filters in the discrete spatial frequency domain. The dashed curve indicates the sum of all filters.

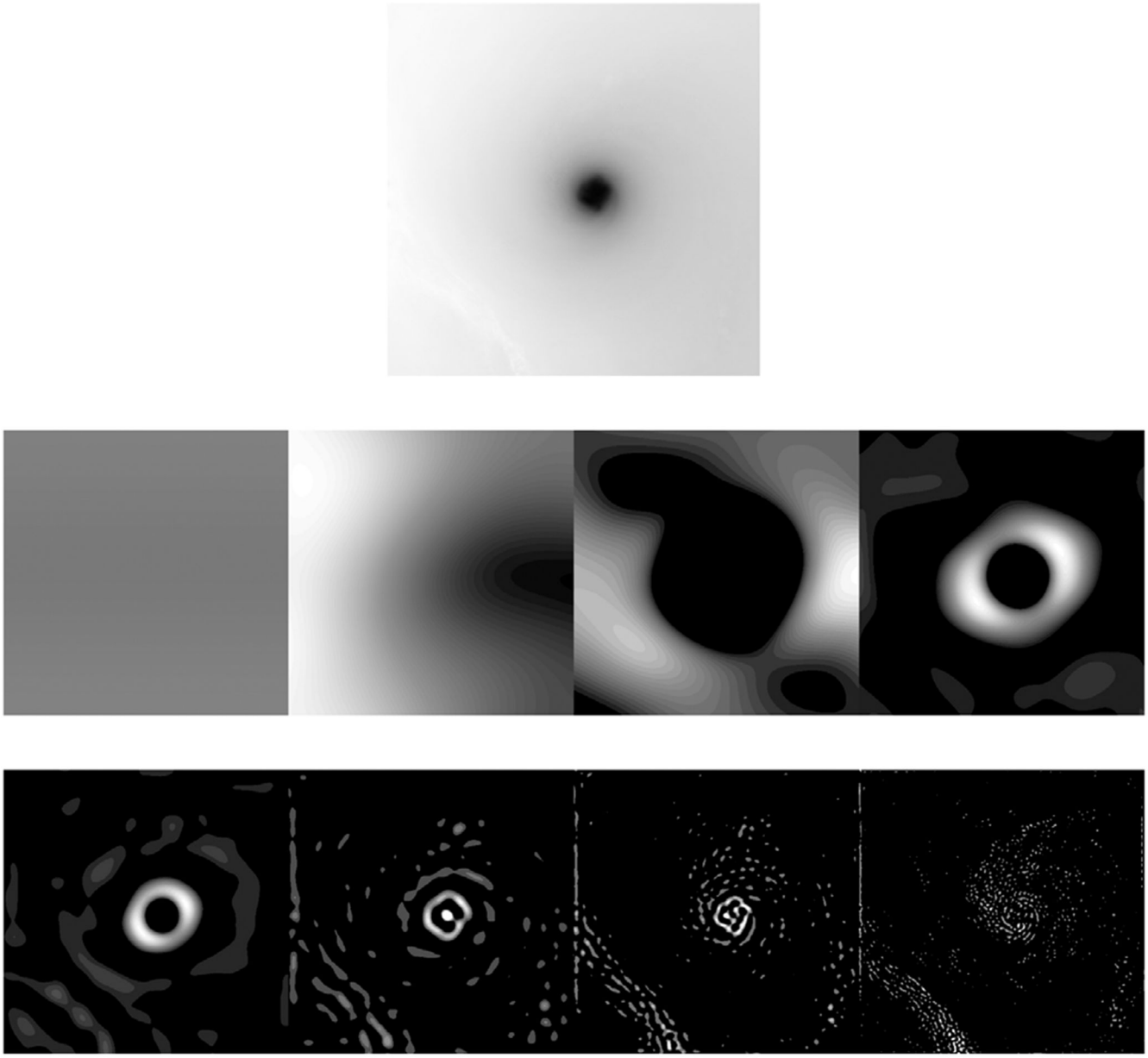

Fig. 4.

Cosine-log image pyramid of a visualization of the Hurricane Isabel dataset. The input image is shown on the top row; images in the pyramid are shown with increasing spatial frequency from left to right, top to bottom (second and third rows). The bandpass images are amplified for visualization purposes.

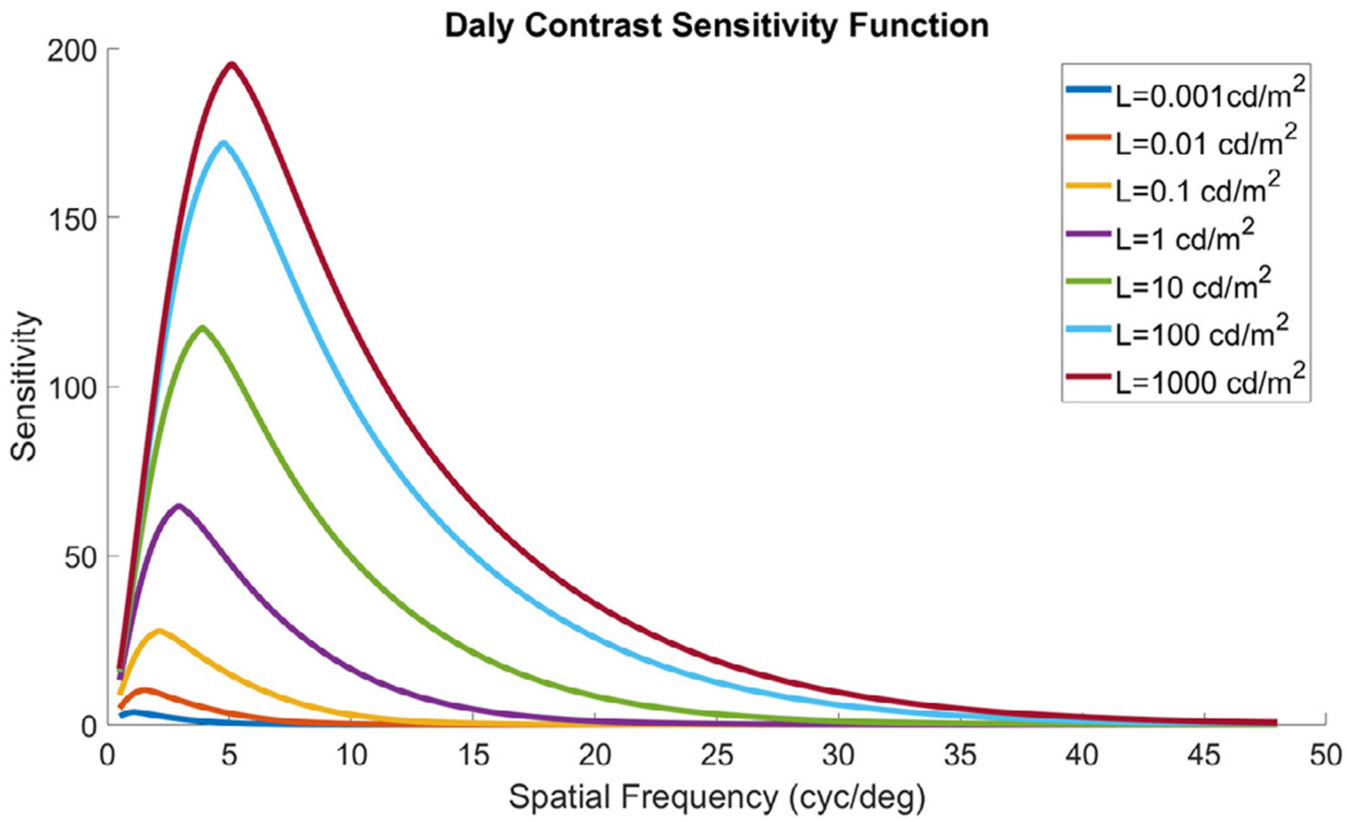

Fig. 5.
Daly CSFs [14] with various illumination levels.

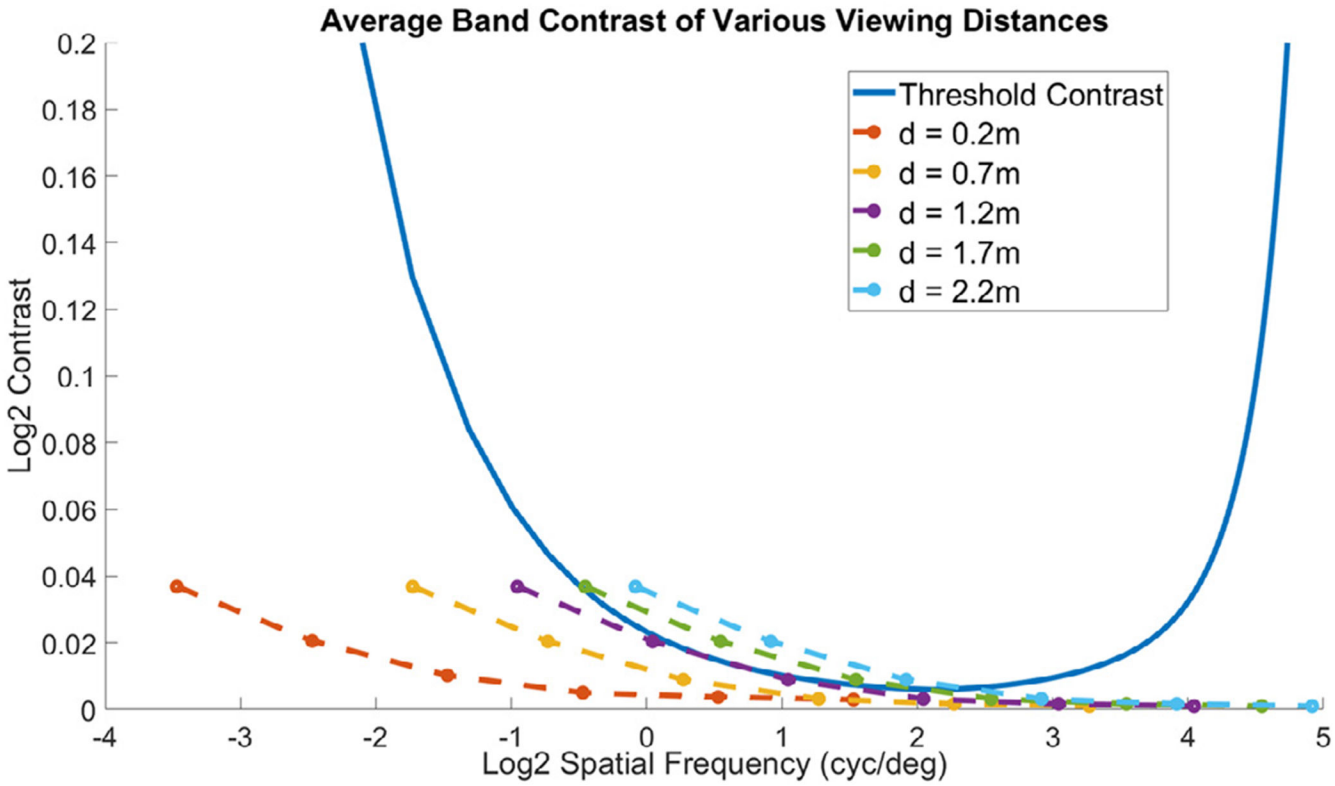

Fig. 6.
Average contrast of various viewing distance with threshold contrast.

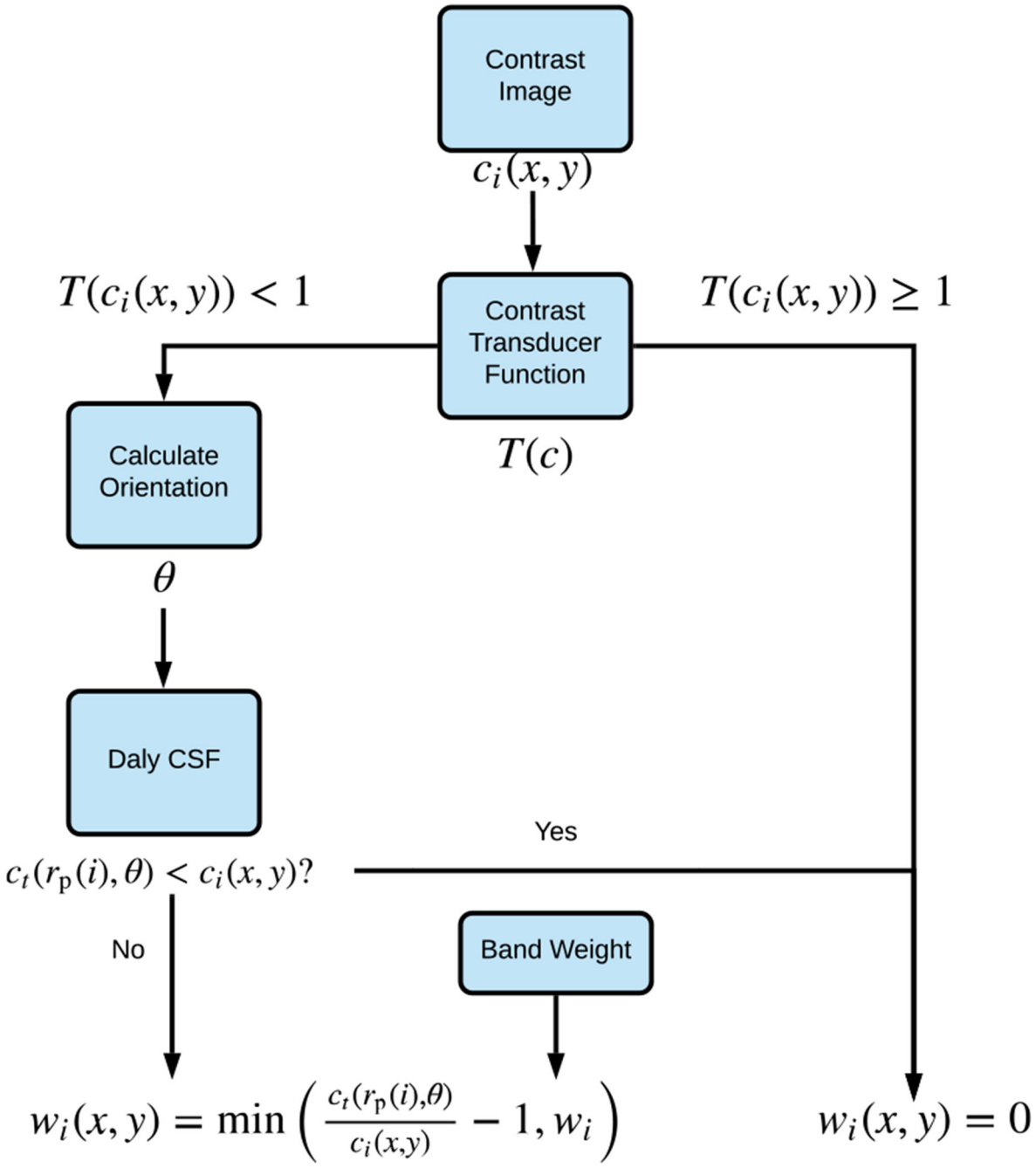

Fig. 7.
The flowchart of pixel-based weight assignment (peak frequency of $c_i(x, y) \leq 32$ cpd).

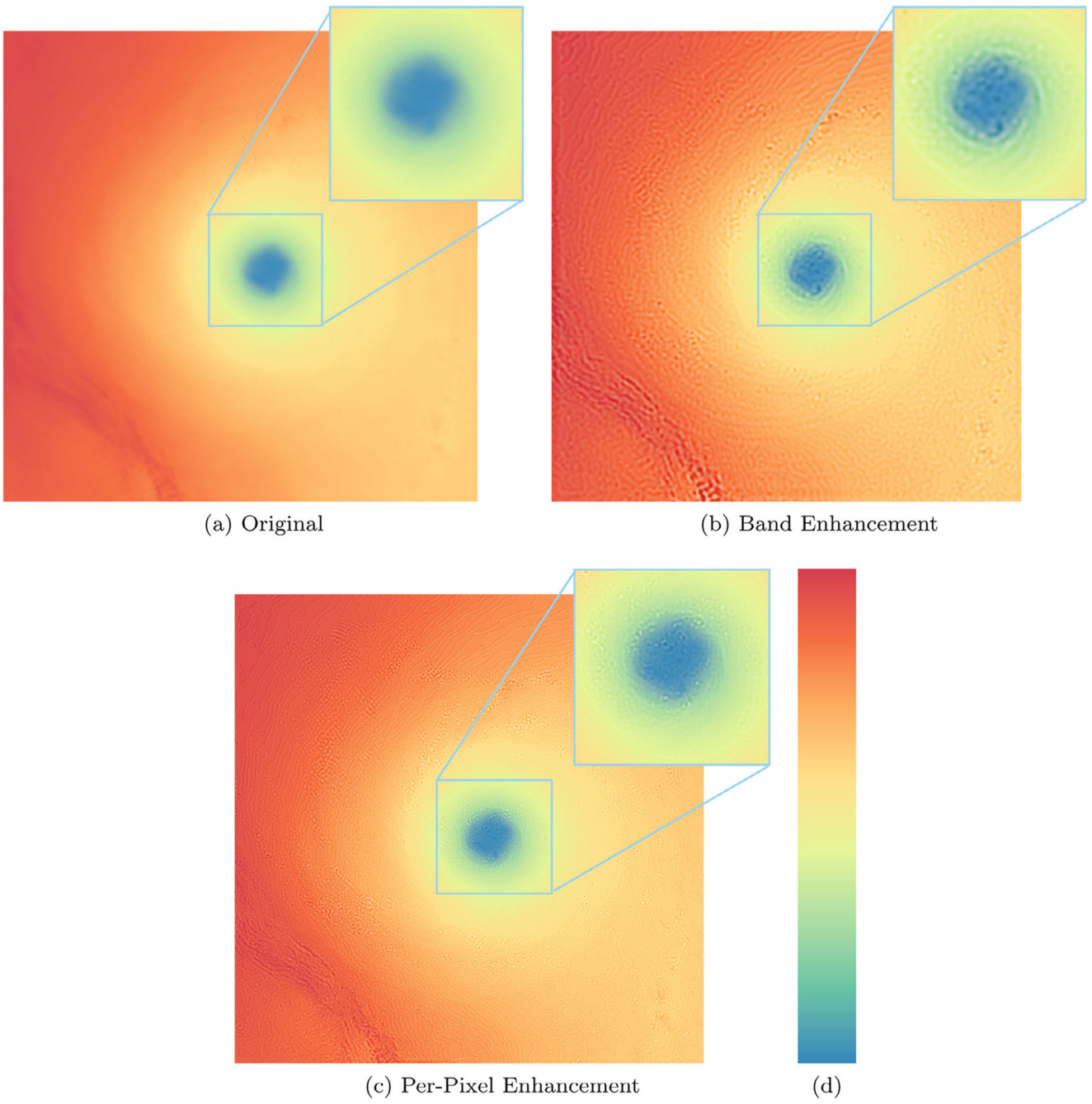

Fig. 8.

Visualizations of the Hurricane Isabel dataset [29]: (a) the original visualization based on a (d) spectrum color map, (b) overcompensated with a viewing distance of 200 cm using the band-based method, and (c) contrast-enhanced by the pixel-based method.

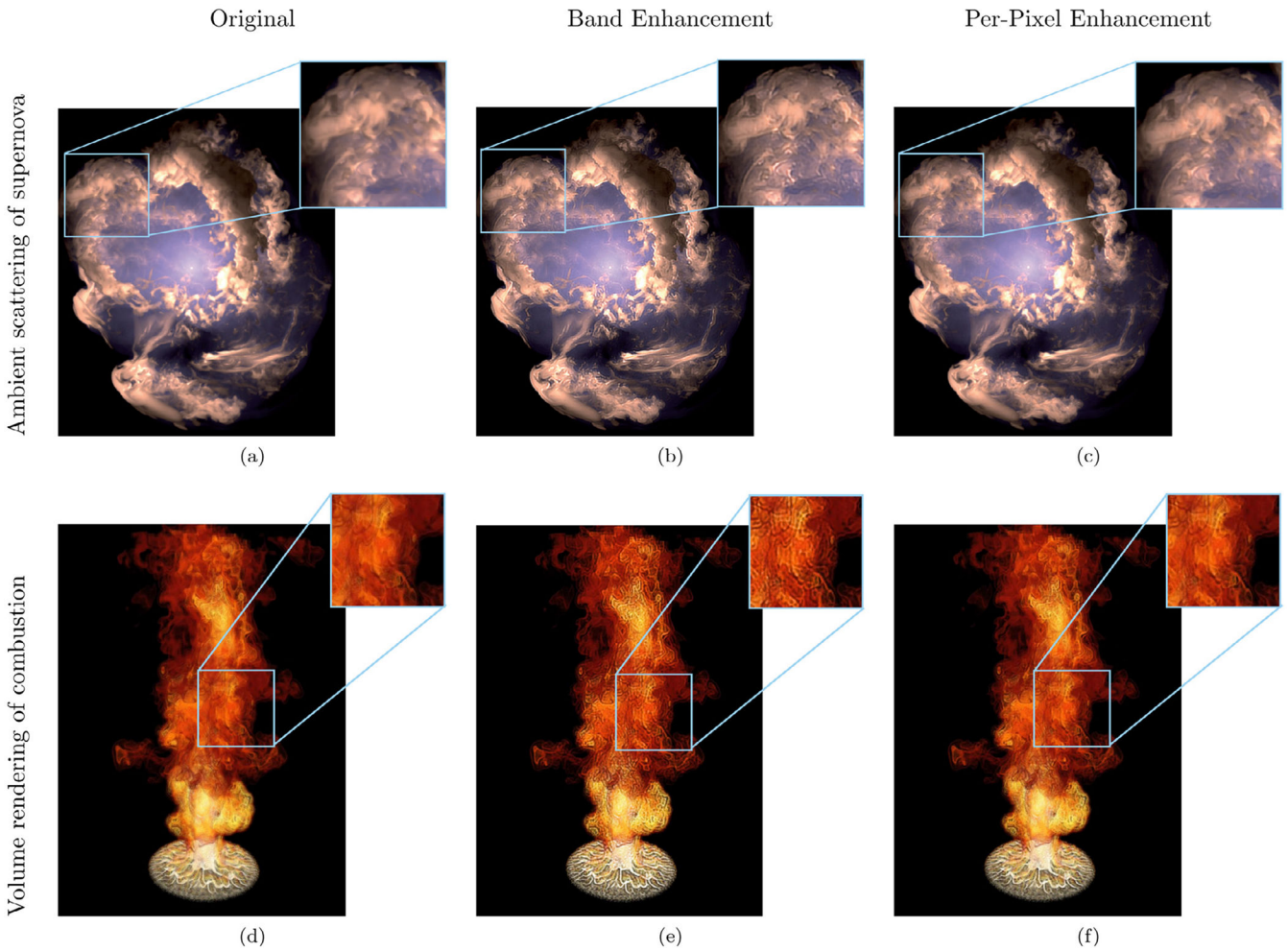

Fig. 9.

Volume renderings with ambient scattering of a supernova dataset are shown in the top row: ©IEEE. Reprinted, with permission, from Ament et al. [30]. Phong-shaded volume renderings of a combustion simulation are shown in the bottom row: ©SCI institute. Reprinted, with permission. The original images are shown in the left column, band-based enhancements are shown in the central column, and pixel-based enhancements are shown in the right column.

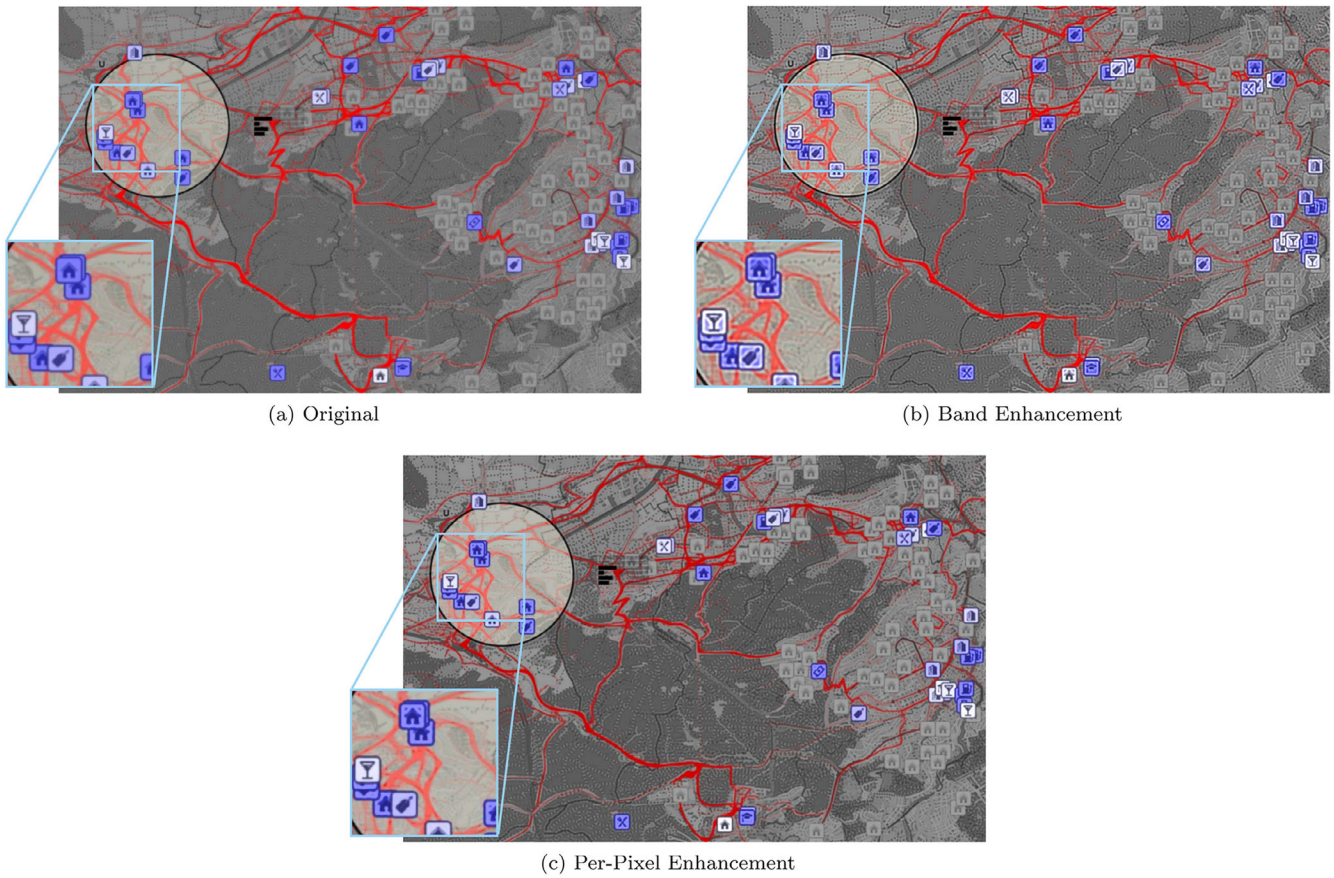

Fig. 10.

Visualization of a GIS dataset: the original image (a) is contrast enhanced by the band-based method (b) and the pixel-based method (c). ©IEEE. Reprinted, with permission, from Krueger et al. [31].

Table 1

The exponent p for various peak spatial frequencies in Eq. (10).

Freq (cpd)	0.5	1.0	2.0	4.0	8.0	16.0	32.0
p	1.93	1.35	1.15	1.04	1.15	1.40	2.63

Table 2

Quantitative metrics of the original visualizations, enhancements with band-based method, and enhancements with pixel-based method.

Dataset	s_o	s_{be}	s_{pe}	i_{be}	i_{pe}
Supernova	46.6867	42.0056	39.7383	0.9748	0.9954
MRI	40.7385	43.4585	21.3608	0.9696	0.9982
Isabel	49.9857	42.8227	49.2977	0.9813	0.9913
HE	51.6422	49.3146	50.5710	0.9928	0.9977
GIS	35.0151	48.6560	44.4159	0.9313	0.9510